

## Prey Switching with a Linear Preference Trade-Off\*

Sofia H. Piltz<sup>†</sup>, Mason A. Porter<sup>‡</sup>, and Philip K. Maini<sup>§</sup>

**Abstract.** In ecology, *prey switching* refers to a predator’s adaptive change of habitat or diet in response to prey abundance. In this paper, we study piecewise-smooth models of predator-prey interactions with a linear trade-off in a predator’s prey preference. We consider optimally foraging predators and derive a model for a 1 predator-2 prey interaction with a tilted switching manifold between the two sides of discontinuous vector fields. We show that the 1 predator-2 prey system undergoes a novel adding-sliding-like (center to two-part periodic orbit; “C2PO”) bifurcation in which the prey ratio transitions from constant to time-dependent. Farther away from the bifurcation point, the period of the oscillating prey ratio doubles, which suggests a possible cascade to chaos. We compare our model predictions with data on freshwater plankton, and we successfully capture the periodicity in the ratio between the predator’s preferred and alternative prey types. Our study suggests that it is useful to investigate prey ratio as a possible indicator of how population dynamics can be influenced by ecosystem diversity.

**Key words.** Lotka–Volterra interaction, Filippov systems, adding-sliding bifurcation, planktonic protozoa-algae dynamics

**AMS subject classifications.** 37N25, 92B05, 34C23, 37G15

**DOI.** 10.1137/130910920

**1. Introduction.** Ciliates are a type of *protist* (i.e., eukaryotic single cell with animal-like behavior) that propel themselves using an undulating movement that is generated by small hair-like protuberances (called *cilia*) that cover the cell body. They are also *planktonic*,<sup>1</sup> as they are transported primarily by currents. Ciliates occur in aquatic environments and feed on small phytoplankton, so they constitute an important link between the bottom and higher levels of marine and freshwater food webs [43]. We have studied data from observations for ciliates and their algal prey collected from Lake Constance on the German-Swiss-Austrian border [41, 42]. As observed in several other ecosystems, the Lake Constance data exhibit

---

\*Received by the editors February 25, 2013; accepted for publication (in revised form) by B. Sandstede January 6, 2014; published electronically April 17, 2014. The Lake Constance data in this work were provided by Ursula Gaedke and obtained within the Collaborative Programme SFB 248 funded by the German Science Foundation.

<http://www.siam.org/journals/siads/13-2/91092.html>

<sup>†</sup>Oxford Centre for Industrial and Applied Mathematics, Mathematical Institute, University of Oxford, Andrew Wiles Building, Radcliffe Observatory Quarter, Woodstock Road, Oxford, OX2 6GG, UK ([sofia.piltz@linacre.ox.ac.uk](mailto:sofia.piltz@linacre.ox.ac.uk)). The work of this author was supported by the Osk. Huttunen Foundation and Engineering and Physical Sciences Research Council through the Oxford Life Sciences Interface Doctoral Training Centre.

<sup>‡</sup>Oxford Centre for Industrial and Applied Mathematics, Mathematical Institute, University of Oxford, Andrew Wiles Building, Radcliffe Observatory Quarter, Woodstock Road, Oxford, OX2 6GG, UK, and CABDyN Complexity Centre, University of Oxford, Oxford, OX1 1HP, UK ([porterm@maths.ox.ac.uk](mailto:porterm@maths.ox.ac.uk)).

<sup>§</sup>Wolfson Centre for Mathematical Biology, Mathematical Institute, University of Oxford, Andrew Wiles Building, Radcliffe Observatory Quarter, Woodstock Road, Oxford, OX2 6GG, UK, and CABDyN Complexity Centre, University of Oxford, Oxford, OX1 1HP, UK ([maini@maths.ox.ac.uk](mailto:maini@maths.ox.ac.uk)).

<sup>1</sup>We have chosen to follow the generally accepted convention of using “planktonic” instead of *planktic*, which is the technically correct adjective.

coexistence of predators and multiple prey. Importantly, ciliates and their algal prey populations also vary at shorter-than-seasonal temporal scales. During years when the spring bloom lasts for several weeks (equivalent to 15 to 30 ciliate generations), phytoplankton and ciliate biomasses exhibit recurring patterns of increases followed by declines [43].

Coexistence of species in a shared environment can arise from ecological *trade-offs* [22]. For example, because of limited resources, an organism that invests energy in feeding strategies of one type of prey cannot invest as much energy in specialized feeding of another type of prey. Similar trade-offs are ubiquitous in ecology, and another example is the trade-off between predator defense mechanisms and high growth rate in phytoplankton [30]. Additionally, previous research suggests that a predator's adaptive change of diet or habitat in response to prey abundance is a possible mechanistic explanation for coexistence [24, 2]. There have been many investigations of *prey switching* [32], in which predators express preference for more abundant prey. For example, it has been demonstrated that prey switching promotes coexistence of competing prey species [40] and to decrease prey competition due to a shared predator [1]. Moreover, prey preference and selective feeding in predator behavior has also been observed in a laboratory experiment on ciliate predator and phytoplankton prey species found in Lake Constance [31]. Because of such studies, it has been suggested that the driving forces for the subseasonal temporal variability observed in ciliate-algal dynamics lie in predator-prey interactions between diverse predator and prey plankton communities—particularly during periods of the year in which environmental conditions are relatively settled [44].

Typically, two prey species (with limited growth) coexist if they share a predator. However, a standard Lotka–Volterra model for one predator and two prey (with unlimited prey growth) that allows diversity in the prey community predicts extinction of the prey type that has a smaller capacity to survive [23]. Therefore, such a framework is inappropriate for investigations of ciliate-phytoplankton dynamics during spring when predator-prey interaction—rather than nutrient limitation—seems to govern plankton dynamics [44, 36], and several predators and prey coexist. Furthermore, there is a known preference towards one of the phytoplankton prey [31]. In smooth differential-equation models for population dynamics, one can model prey switching, which arises as a change in predation of one prey type as opposed to a predator alternating between several prey types, using a Holling type-III functional response [19], in which predation is low at low prey densities but saturates quickly at a high value when prey is abundant. Such a functional response was observed in a system of protist predators and their yeast prey [16]. One can explicitly examine predator preference towards more abundant prey by constructing models with multiple prey in which the densities of the different prey are system variables. This approach has been employed when switching is independent of total prey density, for density-dependent switching [2], and when using information on which prey type was consumed last when there are two [48] or more [47] prey.

An alternative approach to studying prey switching is to posit that predators behave as *optimal foragers* instead of explicitly incorporating adaptive predator behavior in response to changing prey densities. According to *optimal foraging theory*, a predator's choice to switch prey depends on prey abundances and which diet composition maximizes its rate of energy intake [38]. Optimal foraging theory is based on constant population densities, and it aims to predict when a predator will always feed on its preferred prey. An optimal forager also feeds on an alternative prey if doing so does not decrease its rate of energy intake

[38]. Křivan [24] showed that an alternative prey can be part of an optimal forager's diet (such that the probability that the predator attacks the alternative prey is  $p \in [0, 1]$ ). By contrast, the corresponding 1 predator-2 prey system in which the predator is not an optimal forager predicts that both prey coexist and that the predator becomes extinct. It has also been demonstrated that optimal foraging reduces population-density oscillations compared to models with nonadaptive predators [28, 6, 27]. In addition to the choice of whether to include or exclude an alternative prey, similar models of optimal behavior in 1 predator-2 prey systems have been built to study adaptive change of habitat in a two-patch environment [25] as well as adaptive change of activity level [26].

When using the principle of optimal foraging, a 1 predator-2 prey interaction can be modeled as a discontinuous dynamical system. In this paper, we construct a model using the theory of *piecewise-smooth dynamical systems*, which are a class of discontinuous dynamical systems [5, 8] in which continuous temporal evolution of state variables alternates with abrupt events that can be caused by friction, collisions, impacts, switching relays, etc. In addition to engineering applications, piecewise-smooth dynamical systems have also been used in some applications in biology. For example, they have been used in population dynamics for the prey switching discussed above as well as to analyze the effects on predator-prey population dynamics if a predator population is not allowed to be harvested when it is rare [12, 29]. Additionally, piecewise-linear dynamical systems have been used to approximate Hill functions in models of gene regulatory networks [17, 7] and to describe and quantify synchronization of cattle [39].

In the present paper, we aim to provide a possible mechanistic explanation for predator-prey coexistence in the presence of prey preference, which has been observed between ciliate and phytoplankton populations in Lake Constance [43, 44]. We apply optimal foraging theory to derive a piecewise-smooth dynamical system that models a predator that feeds adaptively on its preferred prey and an alternative prey. We propose that the predator has two different feeding modes of the preferred prey; and the predator behavior is adaptive in the sense that it can choose, depending on the prey densities, to consume the preferred prey either with a large or with a small preference. For simplicity, we assume that consuming a small amount of the preferred prey amounts to not consuming it at all. Consequently, when choosing to consume the preferred prey to a small extent, the predator feeds only on the alternative prey. Similarly, when the predator chooses to feed on the preferred prey with a large preference, the alternative prey is not being predated at all. We take two ecological trade-offs into account. First, we introduce a linear trade-off in the parameter that represents the prey preference. Thus, an increase in growth in the predator population as a result of feeding on the preferred prey comes at a cost of the energy obtained from the alternative prey. Second, to compensate for the preference, we assume that the preferred prey has the advantage of a higher growth rate than that of the alternative prey. We examine the outcome of the population dynamics in such a discontinuous 1 predator-2 prey system as we adjust the steepness of the linear dependence of the preference trade-off. We thereby discover a previously unknown (at least to our knowledge) bifurcation in piecewise-smooth dynamical systems and provide a possible link between predator-prey dynamics and ecological trade-offs.

The remainder of this paper is organized as follows. In section 2, we discuss the Lake Constance data set. In section 3.1, we derive a piecewise-smooth dynamical system for an

optimally foraging predator and two prey in the presence of prey preference trade-off. In such a piecewise-smooth system, a switching manifold divides phase space into two smooth parts and marks the transition between them. On the switching manifold, the right-hand side of the piecewise-smooth dynamical system is not uniquely defined. However, a unique solution can be constructed either using Utkin's equivalent control method [46] or Filippov's convex method [13]. In addition, piecewise-smooth dynamical systems can exhibit a rich set of behaviors that are not encountered in smooth dynamical systems. Such behavior includes equilibria located on the switching manifold, dynamics governed by the flow at the switching manifold, and discontinuity-induced bifurcations. In section 3.2, we investigate the 1 predator-2 prey system analytically. We derive the flow at the switching boundary using Filippov's method. We also present analytical expressions for the equilibrium point at the switching boundary and for the points at which the two vector fields on the different sides of the boundary are tangent to the switching boundary between them. In section 3.3, we investigate the 1 predator-2 prey system numerically. We examine the dynamics as we adjust the slope of the preference trade-off and discover a previously unknown bifurcation in piecewise-smooth systems. This (center to two-part periodic orbit; "C2PO") bifurcation describes a transition between a center located entirely on the switching boundary and a periodic orbit that evolves partly along the boundary and partly outside of it. As the distance to the bifurcation point increases, the periodic orbit experiences a period-doubling, which suggests a possible cascade to chaos. In section 3.4, we compare simulations of our system with data on planktonic protozoa-algae dynamics. We discuss and comment on our model assumptions, results, and possible generalizations in section 4 before concluding in section 5.

**2. Lake Constance data.** Lake Constance is a freshwater lake, with a surface area of 536 km<sup>2</sup>, that is situated on the German-Swiss-Austrian border. It has been under scientific study for decades, and hourly records of weather conditions—such as temperature, surface irradiance, and wind speed—have been collected since 1979. In addition to such abiotic factors, weekly data on biomass of several phytoplankton and zooplankton species are also available [3].

In its natural state, Lake Constance would be categorized as a lake with a low level of productivity if there were no excess nutrients from agricultural and other sources of human population in its catchment area. However, the increased sewage-water treatment since 1979 has reduced the amount of nutrients that enter Lake Constance, which was categorized as a lake with an intermediate level of productivity (as measured in terms of abundance of nutrients such as nitrogen and phosphorus) when the data were collected [44]. Nowadays, Lake Constance is once again categorized as a lake with a low level of productivity. In our comparison between model simulations and data in section 3.4, we will consider the biomass data for the algal prey of protozoan predators until 1999 that were reported previously in [41, 42]. We concentrate on the early growth season, during which the population dynamics are governed predominantly by predator-prey interactions rather than by factors such as population dilution from increased mixing between the upper and lower water masses or strong predation of protists by carnivorous zooplankton populations (which develops later in the season) [37, 44].

The data that we received include abundance (individuals or cells per ml) and biomass

(units of carbon per  $\text{m}^2$ ) of a species obtained at least once in a sample of a few ml to a liter of water in Lake Constance between March 1979 and December 1999. When unavailable, the abundance or the biomass were calculated from each other using species size as a conversion factor [41, 42]. Each sample was collected from a water column with an area of  $1 \text{ m}^2$  and a depth of 20 m. The full data set includes over 23,000 observations of 205 different phytoplankton species. We used a subset of these data for the comparison in section 3.4. In particular, we selected phytoplankton species that were noted in [44] as representative species for preferred and alternative prey of ciliate predators.

### 3. Piecewise-smooth 1 predator-2 prey model.

**3.1. Equations of motion.** We begin the construction of a model for a predator and its preferred and alternative prey by assuming a linear trade-off between the preference towards the preferred and alternative preys. In our framework, prey switching occurs because the predator can adjust the extent of consumption of the preferred prey. The trade-off in the prey preference is effectively a trade-off in how much energy the predator gains from eating the preferred prey instead of the alternative prey. An increase in specialization towards the preferred prey comes at a cost of the predator population growth obtained from feeding on the alternative prey. For simplicity, we assume that the preference trade-off is linear:

$$(3.1) \quad q_2 = -a_q q_1 + b_q,$$

where  $q_1 \geq 0$  is a nondimensional parameter that represents the desire to consume the preferred prey,  $a_q > 0$  is the slope of the preference trade-off,  $b_q \geq 0$  is the intercept of the preference trade-off, and  $q_2 \geq 0$  is the desire to consume the alternative prey. Assuming a linear predator mortality and a linear functional response between the predator growth and prey abundance, we define a fitness function that the predator maximizes using the net per capita growth rate

$$(3.2) \quad R \equiv \frac{1}{z} \frac{dz}{dt} = e q_1 \beta_1 p_1 + e q_2 \beta_2 p_2 - m,$$

where  $z$  is the density of the predator population,  $p_1$  is the density of the preferred prey,  $p_2$  is the density of the alternative prey,  $e > 0$  is the proportion of predation that goes into predator growth,  $\beta_1$  and  $\beta_2$  are the respective death rates of the preferred and alternative prey due to predation, and  $m > 0$  is the predator per capita death rate per day.

We obtain the switching condition that describes when the predator chooses consumption with a large preference towards the preferred prey ( $q_1 = q_{1L}$ ) or consumption with a small preference towards the preferred prey ( $q_1 = q_{1S}$ ) to maximize fitness by substituting (3.1) into (3.2) and differentiating  $R$  with respect to  $q_1$ :

$$(3.3) \quad \frac{\partial R}{\partial q_1} = (\beta_1 p_1 - a_q \beta_2 p_2) e.$$

Thus, when  $\frac{\partial R}{\partial q_1} > 0$ , the largest feasible  $q_{1L}$  maximizes predator fitness; when  $\frac{\partial R}{\partial q_1} < 0$ , the smallest feasible  $q_{1S}$  maximizes predator fitness. For simplicity, we assume that  $q_{1S} = 0$ . This implies that the predator switches to the feeding mode of consuming only the alternative prey

when predator fitness is maximized by having a small preference for consuming the preferred prey. We also assume (again for simplicity) that prey growth is exponential. This yields the following piecewise-smooth 1 predator-2 prey model:

$$(3.4) \quad \dot{\mathbf{x}} = \begin{bmatrix} \dot{p}_1 \\ \dot{p}_2 \\ \dot{z} \end{bmatrix} = \begin{cases} f_+ = \begin{bmatrix} (r_1 - \beta_1 z)p_1 \\ r_2 p_2 \\ (eq_1 \beta_1 p_1 - m)z \end{bmatrix} & \text{if } h = \beta_1 p_1 - a_q \beta_2 p_2 > 0 \\ f_- = \begin{bmatrix} r_1 p_1 \\ (r_2 - \beta_2 z)p_2 \\ (eq_2 \beta_2 p_2 - m)z \end{bmatrix} & \text{if } h = \beta_1 p_1 - a_q \beta_2 p_2 < 0 \end{cases},$$

where  $h = \beta_1 p_1 - a_q \beta_2 p_2 = 0$  determines the switching manifold and  $r_1 > r_2 > 0$  are the per capita growth rates of the preferred ( $r_1$ ) and alternative ( $r_2$ ) prey. The right-hand side of (3.4) cannot be determined uniquely for  $h = 0$  by the criterion based on optimal foraging theory. For this part of the phase space, the flow at the discontinuity must be constructed from  $f_+$  and  $f_-$ . We will specify (3.4) at the switching manifold in (3.10).

In our numerical simulations in section 3.3, we take  $\beta_1 = \beta_2$ . (For simplicity, we also take  $\beta_1 = \beta_2 = 1$  in order to omit  $\beta_1$  and  $\beta_2$  in our analysis in section 3.2.) Hence, we assume that the predator exhibits adaptive feeding behavior by adjusting its preference toward—rather than its attack rate on—the governing prey densities. We can use production-to-biomass ratio, where the biomass is the mass of all living and dead organic matter and production represents the increase in biomass produced by phytoplankton organisms, calculated from measurements in Lake Constance (see section 2) as an index for phytoplankton growth. These data suggest that typical values for the phytoplankton per capita growth rate vary approximately from 0.2 per day to 0.6 per day during the course of a year.

Because of the prey preference, the predator exerts more grazing pressure on the preferred prey than on the alternative prey. One can explain this advantage for the alternative prey by a difference in the use of limited nutrients. For example, the alternative prey might invest resources in building defense mechanisms such as a hard silicate cover, which is difficult for the predator to digest. As a result, the alternative prey has fewer resources left for population growth than the preferred prey (which does not have as good a defense against the predator). To compensate for the difference in preference, we assume that the growth rate of the preferred prey is larger than that of the alternative prey.

Our 1 predator-2 prey model assumes that the switch from the preferred prey to the alternative prey occurs instantaneously. It is reasonable to model prey switching via a piecewise-smooth dynamical system as long as predators are assumed to behave as optimal foragers. The discontinuity in (3.4) comes from using the principle of optimal foraging theory [38], which states that a predator chooses a diet that maximizes its growth. Hence, to determine the optimal choice for consumption, we differentiate the mean energy intake rate with respect to the prey preference, which is the parameter that the predator can adjust. It is not clear whether there exist “discontinuous predators” (which switch their feeding strategy instantaneously, as is the case in our model). To our knowledge, however, there is no evidence for any of the possible smooth approximations that one can choose to model prey switching. Therefore, we use an abrupt switch rather than a gradual switch and focus on a model with a discontinuity.

**3.2. Analysis of the 1 predator-2 prey model.** In this section, we review some definitions from piecewise-smooth dynamical systems and then examine their manifestation in the 1 predator-2 prey system (3.4). We will verify our analytical results (and also obtain additional insights) using numerical simulations in section 3.3.

**3.2.1. Basic definitions from piecewise-smooth dynamical systems.** The piecewise-smooth 1 predator-2 prey system with Lotka–Volterra interaction terms in (3.4) contains a discontinuity in the derivative of the population densities across the discontinuity boundary  $h = 0$ . This discontinuity makes (3.4) a *Filippov system*. Note that piecewise-smooth dynamical systems can be categorized by their *degree of smoothness*, which is defined as the highest order  $r$  such that the Taylor series expansions of  $\phi_+(x_0, t)$  and  $\phi_-(x_0, t)$  with respect to  $t$ , evaluated at  $t = 0$ , agree up to terms of  $\mathcal{O}(t^{r-1})$ . The quantities  $\phi_+$  and  $\phi_-$  are smooth flows defined, respectively, by  $f_+$  and  $f_-$ ; and  $x_0$  is a point on the switching manifold  $h = 0$ . From the definition above, the degree of smoothness is given by the first nonzero partial derivative with respect to  $t$  of the difference  $[\phi_+(x_0, t) - \phi_-(x_0, t)]|_{t=0}$  [5]. Filippov systems such as the one in (3.4) have a degree of smoothness equal to 1. Because of the jump in the derivative, Filippov systems allow the possibility for the dynamics to evolve towards the switching manifold from both sides of the discontinuity.

As we show in Figure 1, the orientation of the vector fields  $f_+$  and  $f_-$  determines whether the switching manifold is attracting or repelling. Three types of associated dynamics can occur near a switching manifold in a piecewise-smooth system. When the switching boundary is attracting from both sides of the discontinuity, the system is said to exhibit *sliding* [panel (a)]. *Crossing* occurs when trajectories that start from one side of the discontinuity traverse the switching boundary without following the sliding field on the boundary [panel (b)]. If both of the vector fields point outward from the discontinuity, then the region is defined as a region in which *escaping* occurs [panel (c)].

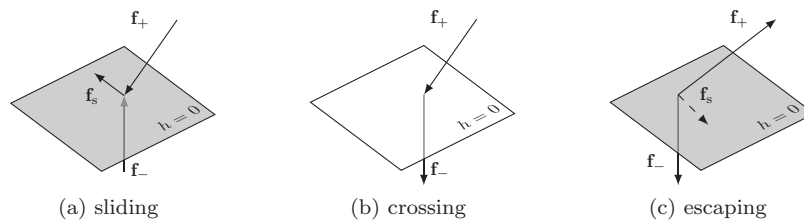


**Figure 1.** The three possible types of dynamics in a piecewise-smooth system close to the switching manifold  $h = 0$ : (a) sliding along the sliding vector field  $f_s$ , (b) crossing, and (c) escaping (i.e., unstable sliding).

The boundaries of sliding, crossing, and escaping are determined by computing the points at which there is a tangency between the vector fields  $f_-$  or  $f_+$  and the discontinuity boundary  $h = 0$  (see Figure 2). Determining the tangencies is crucial for studying the behavior of a system near a switching boundary, and it constitutes the first step for studying how dynamics in a piecewise-smooth dynamical system differ from that in a smooth dynamical system [9].

There are three basic tangencies between a piecewise-smooth vector field and a switching boundary. In a *fold*, a vector field has a quadratic tangency with a switching boundary [see Figure 2(a)]. In a *cusp*, the tangency is cubic [see Figure 2(b)]. Finally, a *two-fold* occurs when

two folds intersect, and there is a quadratic tangency between a switching manifold and each side of a vector field [see Figure 2(c)]. In section 3.2.5, we will determine the points at which one of the vector fields in (3.4) has a cubic or quadratic tangency with the switching boundary  $h = p_1 - a_q p_2 = 0$ . Although a two-fold can arise in three-dimensional piecewise-smooth dynamical systems, it does not occur in (3.4) because the crossing and sliding boundaries do not intersect on the switching manifold. We will derive the regions of crossing and sliding in section 3.2.2.

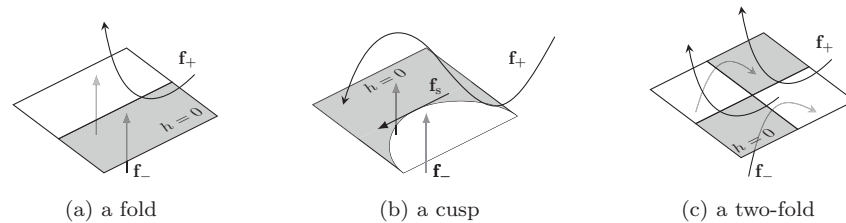


**Figure 2.** Three basic tangencies between a piecewise-smooth vector field and a switching manifold occur at (a) a fold (i.e., a quadratic tangency), (b) a cusp (i.e., a cubic tangency), and (c) a two-fold (i.e., an intersection of two folds). [We have shaded the sliding and escaping regions.]

Studying the aforementioned tangencies in a piecewise-smooth system makes it possible to describe bifurcations that can occur when, for example, a limit cycle or an equilibrium point intersects a tangency point on a switching boundary. Such bifurcations are examples of *discontinuity-induced bifurcations* (DIBs) [5]. In particular, in a system with three or more dimensions, such as the 1 predator-2 prey system (3.4), all generic one-parameter sliding bifurcations occur at either a fold, a cusp, or a two-fold. Moreover, because the switching manifold  $h = 0$  in (3.4) has codimension 1, all of its one-parameter sliding bifurcations can be categorized into eight different cases (depending on the type of the tangency) [20].

If there is a cusp, a trajectory that is situated entirely in the sliding region has a tangency with the boundary. That is, the sliding vector field has a quadratic tangency to the switching boundary. Perturbing the bifurcation parameter from the bifurcation point results in the sliding trajectory leaving the switching plane tangentially; because of the cubic tangency with the vector field, it returns to the sliding region. This is called an *adding-sliding* bifurcation because a trajectory that was entirely a sliding trajectory becomes a trajectory that now includes both a nonsliding segment and a sliding segment [5]. A new sliding segment is thereby added to the trajectory.

In the next four subsections, we determine the regions of sliding, crossing, and escaping for (3.4); derive the analytical expression for the sliding flow that is the solution to (3.4) at the boundary  $h = 0$ ; calculate the equilibrium point and associated eigenvalues of the sliding vector field; and compute analytical expressions for points at which there is either a quadratic or a cubic tangency between one of the vector fields and the switching boundary.

**3.2.2. Regions of sliding, crossing, and escaping.** The regions in which (3.4) undergoes sliding or escaping are located where the component of  $f_+$  normal to  $h = 0$  has the opposite sign to the component of  $f_-$  normal to  $h = 0$ . The switching boundary is then either attracting or repelling from both sides of the boundary. The condition for sliding or escaping to occur

in (3.4) is

$$(3.5) \quad \mathcal{L}_{f_+} h \mathcal{L}_{f_-} h = (a_q p_2)^2 [(r_1 - r_2)^2 - z^2] < 0,$$

where  $\mathcal{L}$  denotes the Lie derivative along the flow  $f$  and is defined for  $f_+$  as  $\mathcal{L}_{f_+} = f_+ \cdot \nabla = \dot{\mathbf{x}}|_{f_+} \cdot \frac{d}{d\mathbf{x}}$ . It is defined analogously for  $f_-$ . Thus, either sliding or escaping occurs in (3.4) for  $z^2 > (r_1 - r_2)^2$ . When  $z^2 < (r_1 - r_2)^2$ , a solution of (3.4) crosses the switching boundary because the components of  $f_+$  and  $f_-$  normal to  $h = 0$  have the same sign. Therefore, trajectories that start from one side of the boundary pass through  $h = 0$  without evolving along it.

In stable sliding regions, the components of both  $f_+$  and  $f_-$  that are normal to  $h = 0$  point towards the switching manifold, and trajectories reach sliding motion in finite time. This occurs in (3.4) when

$$(3.6) \quad \mathcal{L}_{f_+} h < 0 < \mathcal{L}_{f_-} h \implies -z < r_1 - r_2 < z.$$

Escaping (i.e., unstable sliding) occurs because the components of both  $f_+$  and  $f_-$  that are normal to  $h = 0$  point away from  $h = 0$ . Trajectories that reach these regions are repelled from the switching manifold in finite time. Escaping motion is unattainable in simulations in forward time. Escaping occurs in (3.4) when

$$(3.7) \quad \mathcal{L}_{f_+} h > 0 > \mathcal{L}_{f_-} h \implies -z > r_1 - r_2 > z.$$

**3.2.3. Sliding vector field.** The solution to (3.4) at the discontinuity  $h = 0$  can be expressed using Filippov's differential inclusion [13]. According to Filippov's method, the flow of (3.4) at  $p_1 = a_q p_2$  is determined by a linear convex combination of the two vector fields  $f_-$  and  $f_+$  as follows:

$$(3.8) \quad f_s = (1 - \alpha(x))f_- + \alpha(x)f_+,$$

where

$$(3.9) \quad \alpha(x) = \frac{\mathcal{L}_{f_-} h}{\mathcal{L}_{f_-} h - \mathcal{L}_{f_+} h} \in [0, 1].$$

If  $\alpha = 0$ , then the sliding flow  $f_s$  is given by  $f_-$ , so  $h < 0$ . Similarly, if  $\alpha = 1$ , then  $f_s = f_+$ , which implies that  $h > 0$ . Employing (3.8) and (3.9) and looking at  $h = 0$ , we thus see that the dynamics of (3.4) are governed by the sliding vector field

$$(3.10) \quad f_s = \frac{1}{2} \begin{bmatrix} (r_1 + r_2 - z)p_1 \\ (r_1 + r_2 - z)p_2 \\ eq_1 p_1 (r_1 - r_2 + z) + eq_2 p_2 (r_2 - r_1 + z) - 2mz \end{bmatrix} \\ = \frac{1}{2} \begin{bmatrix} (r_1 + r_2 - z)a_q p_2 \\ (r_1 + r_2 - z)p_2 \\ eq_1 a_q p_2 (r_1 - r_2 + z) + eq_2 p_2 (r_2 - r_1 + z) - 2mz \end{bmatrix}.$$

The sliding vector field (3.10) is a linear convex combination of the two vector fields  $f_-$  and  $f_+$  on each side of the switching manifold  $h = p_1 - a_q p_2$ . Equation (3.10) states that both

prey species need to adjust their growth rates to obtain a unique solution on the switching manifold [which we will give in (3.12)]. This is a limitation of the model. The following mechanisms drive the piecewise-smooth system in (3.4) to evolve according to the sliding vector field (3.10). The vector field  $f_-$  points towards the switching manifold for a sufficiently large predator population (for  $z > r_1 - r_2$ ) because the predator prefers prey  $p_1$  (which has an advantage in growth rate compared to the alternative prey), but it can also feed on the alternative prey  $p_2$ . When the predator population is sufficiently small and the predator is feeding on the alternative prey (i.e., when  $p_1 - a_q p_2 < 0$ ), the preferred prey population  $p_1$  grows exponentially. As a result, the quantity  $p_1 - a_q p_2$  increases as  $p_1$  becomes more abundant, whereas the population of  $p_2$  decreases because of predation. Consequently, the predator switches to the preferred prey, which also contributes more to predator growth than the alternative prey.

If the predator population is still small (i.e., when  $z < r_1 - r_2$ ) when the switch occurs, then the population of the preferred prey continues to grow after the switch. This, in turn, supports predator growth. At the same time, the population  $p_2$  grows exponentially. However, because of the increasing number of predators that feed on  $p_1$  and the increasing number of alternative prey  $p_2$ , the quantity  $p_1 - a_q p_2$  eventually starts to decrease as predation catches up with the growth of  $p_1$ . At this point,  $f_+$  starts to point towards the switching manifold. The vector field  $f_-$  also points towards the switching manifold because the population of the alternative prey  $p_2$  (if it is being eaten by the predator) would decrease in the presence of a large predator population. Hence, at the switching manifold in the sliding region (i.e., when  $z > r_1 - r_2$ ), the predator is feeding on both prey types because both  $f_-$  and  $f_+$  point towards the switching manifold. In addition, trajectories that enter the switching manifold cannot leave it if the preference trade-off is sufficiently steep. We will discuss the reasons for this phenomenon in sections 3.3.1 and 3.3.2. Consequently, on the switching manifold—for which the dynamics of the system are given by (3.10)—the predator feeds on both prey types and the ratio of the prey populations tends towards  $a_q$ .

The divergence of the sliding vector field is determined by

$$(3.11) \quad \nabla \cdot f_s = \frac{\partial f_s^{(1)}}{\partial p_1} + \frac{\partial f_s^{(2)}}{\partial p_2} + \frac{\partial f_s^{(3)}}{\partial z} = r_1 + r_2 - z + e(q_1 a_q + q_2) p_2 - 2m,$$

where  $f_s^{(i)}$  ( $i \in \{1, 2, 3\}$ ) denotes the  $i$ th component of the sliding flow (3.10).

**3.2.4. The equilibrium point.** The sliding vector field (3.10) has an equilibrium point when  $f_s(\tilde{p}_1, \tilde{p}_2, \tilde{z}) = 0$ . The equilibrium of the sliding flow that is located at the switching boundary is called a *pseudoequilibrium*. For the system (3.4), there is a nontrivial pseudoequilibrium point at

$$(3.12) \quad \begin{aligned} \tilde{p}_1 &= \frac{a_q m(r_1 + r_2)}{e(q_1 a_q r_1 + q_2 r_2)}, \\ \tilde{p}_2 &= \frac{m(r_1 + r_2)}{e(q_1 a_q r_1 + q_2 r_2)}, \\ \tilde{z} &= r_1 + r_2. \end{aligned}$$

By evaluating the Jacobian of  $f_s$  at  $(\tilde{p}_1, \tilde{p}_2, \tilde{z})$ , we find that its two eigenvalues are the complex conjugate pair  $\lambda_{1,2}$ , which satisfy the characteristic equation

$$(3.13) \quad \lambda_{1,2}^2 - \frac{m(r_2 - r_1)(q_1 a_q - q_2)}{2(q_1 a_q r_1 + q_2 r_2)} \lambda_{1,2} + \frac{m(r_1 + r_2)}{2} = 0.$$

The eigenvalues  $\lambda_{1,2}$  have negative real parts when  $a_q > q_2/q_1$ , are imaginary when  $a_q = q_2/q_1$ , and have positive real parts when  $a_q < q_2/q_1$ .

**3.2.5. Tangency points.** At the boundary between the sliding and crossing regions, the vector fields  $f_-$  or  $f_+$  become tangent to the switching manifold  $h = p_1 - a_q p_2 = 0$ . At a fold, one vector field has a vanishing first Lie derivative and a nonvanishing second Lie derivative. That is, in the case of a fold for  $f_+$ , we have  $\mathcal{L}_{f_+} h = 0$ , and  $\mathcal{L}_{f_+}^2 h = (\mathcal{L}_{f_+})^2 h \neq 0$ . In addition, the gradient vectors of  $h$  and  $\mathcal{L}_{f_+} h$  must be linearly independent of each other, and the other vector field satisfies  $\mathcal{L}_{f_-} h \neq 0$  [9].<sup>2</sup> The tangency condition for a fold in (3.4) is then

$$(3.14) \quad \mathcal{L}_{f_-} h = \mathcal{L}_{f_+} h = 0 \implies z = \pm(r_1 - r_2).$$

At a cusp, a vector field has a cubic tangency to a boundary. For  $f_+$ , this occurs when both  $\mathcal{L}_{f_+} h = 0$  and  $\mathcal{L}_{f_+}^2 h = 0$ . In addition, the sliding vector field has a quadratic tangency at the sliding boundary. Thus, the conditions  $\mathcal{L}_{f_+}^3 h \neq 0$  and  $\mathcal{L}_{f_-} h \neq 0$  must hold. Additionally, the gradient vectors of  $h$ , the first Lie derivative  $\mathcal{L}_{f_+} h$ , and the second Lie derivative  $\mathcal{L}_{f_+}^2 h$  are required to be linearly independent [9].<sup>3</sup> For  $f_+$  in the 1 predator-2 prey system (3.4), the quadratic tangency is given by

$$(3.15) \quad \mathcal{L}_{f_+}^2 h = a_q p_2 [(r_1 - z)^2 - r_2^2 - z(eq_1 a_q p_2 - m)].$$

Substituting  $\mathcal{L}_{f_+} h = 0$  (i.e.,  $z = r_1 - r_2$ ) into (3.15) yields a cusp at

$$(p_1, p_2, z) = (m/(eq_1), m/(eq_1 a_q), r_1 - r_2).$$

Similarly, the condition for a quadratic tangency for  $f_-$  is

$$(3.16) \quad \mathcal{L}_{f_-}^2 h = a_q p_2 [(r_2 - z)^2 - z(m - q_2 p_2) + r_1^2].$$

Substituting  $\mathcal{L}_{f_-} h = 0$  (i.e.,  $z = r_2 - r_1$ ) into (3.16) yields a cusp at

$$(p_1, p_2, z) = (a_q m/(eq_2), m/(eq_2), r_2 - r_1).$$

<sup>2</sup>Or vice versa, in the case of a fold for  $f_-$ ,  $\mathcal{L}_{f_-} h = 0$ ,  $\mathcal{L}_{f_-}^2 h \neq 0$ , and  $\mathcal{L}_{f_+} h \neq 0$ . The gradient vectors of  $h$  and  $\mathcal{L}_{f_-} h$  must be linearly independent of each other [9].

<sup>3</sup>At a cusp between  $f_-$  and the boundary between sliding and crossing regions,  $\mathcal{L}_{f_-} h = 0$  and  $\mathcal{L}_{f_-}^2 h = 0$ , and the conditions  $\mathcal{L}_{f_-}^3 h \neq 0$  and  $\mathcal{L}_{f_+} h \neq 0$  must hold. In addition, the gradient vectors of  $h$ , the first Lie derivative  $\mathcal{L}_{f_-} h$ , and the second Lie derivative  $\mathcal{L}_{f_-}^2 h$  are required to be linearly independent [9].

**3.3. Numerical simulations.** We now treat the slope  $a_q$  of the preference trade-off as a bifurcation parameter and study the 1 predator-2 prey system (3.4) numerically. We are interested in the dynamics of (3.4) as the complex conjugate pair of eigenvalues of the pseudoequilibrium crosses the imaginary axis.

The parameter  $a_q$  gives the slope of the tilted switching manifold, and it corresponds biologically to the slope of the assumed linear trade-off in the predator's preference for prey. A large  $a_q$  corresponds to a situation in which a small increase in the predator's desire to consume the preferred prey results in a large decrease in its desire for the alternative prey. When  $a_q \rightarrow 0$ , a small specialization in consuming the preferred prey requires only a small decrease in how much energy the predator gains from eating the alternative prey. At  $a_q = 0$ , the preference trade-off no longer decreases (i.e., it is flat), which corresponds to a situation in which specialization in one prey has no effect on the desire for consuming the alternative prey.

We simulate (3.4) numerically in three different cases: (1)  $a_q > q_2/q_1$ , (2)  $a_q = q_2/q_1$ , and (3)  $a_q < q_2/q_1$ . These correspond, respectively, to (1) the complex conjugate pair  $\lambda_{1,2}$  with negative real part, (2) the complex conjugate pair  $\lambda_{1,2}$  with real part 0, and (3) the complex conjugate pair  $\lambda_{1,2}$  with positive real part. To obtain our numerical solutions, we use the method developed in [33] for simulating Filippov systems.

**3.3.1. The equilibrium point.** From our analytical results, we know that the pseudoequilibrium has a complex conjugate pair of eigenvalues with negative real part when  $a_q > q_2/q_1$ . In addition, the divergence of the sliding vector field (3.11) evaluated at the pseudoequilibrium (3.12) is negative. Thus, the pseudoequilibrium behaves as a sink when  $a_q > q_2/q_1$ . Accordingly, numerical simulations of (3.4) in this parameter regime have trajectories that converge to the pseudoequilibrium in (3.12). See Figure 3 for an example trajectory.

**3.3.2. Sliding centers.** At  $a_q = q_2/q_1$ , the complex conjugate pair of eigenvalues  $\lambda_{1,2}$  have a real part equal to 0, and the divergence of the sliding vector field evaluated at the pseudoequilibrium is also 0. Because the pseudoequilibrium is neither attracting nor repelling in the linearized dynamics, every entirely sliding orbit is a periodic orbit that surrounds the pseudoequilibrium (see Figure 4). Thus, the amplitude of a periodic orbit depends on the point at which a trajectory intersects the switching surface. In addition to these sliding periodic orbits, there exist periodic orbits that cross the boundary between sliding and crossing regions, but which initially are not entirely sliding, that converge slowly (with dimensional simulation times on the order of  $10^3$  days or greater) to an entirely sliding periodic orbit that is tangent to the sliding-crossing boundary (see Figure 4).

At the bifurcation point  $a_q = q_2/q_1$ , the dynamics of the system (3.4) on the switching manifold are governed by the two-dimensional sliding vector field (3.10), which is effectively a Lotka–Volterra predator-prey system. Therefore, we can find a first integral of the sliding vector field on the switching manifold to show that (3.10) on  $h = 0$  is a center. We have also done numerical computations of the Lyapunov exponents in the sliding vector field on the switching manifold. Using an implementation by Govorukhin [18] of the algorithm presented in [50] for computing Lyapunov exponents from finite time-series data, we find that the three Lyapunov exponents of the sliding vector field (3.10) on the switching plane converge to 0. At the end of a simulation time of  $10^4$  (nondimensional) units, their values are  $\lambda_1 \approx 1.5 \cdot 10^{-3}$ ,

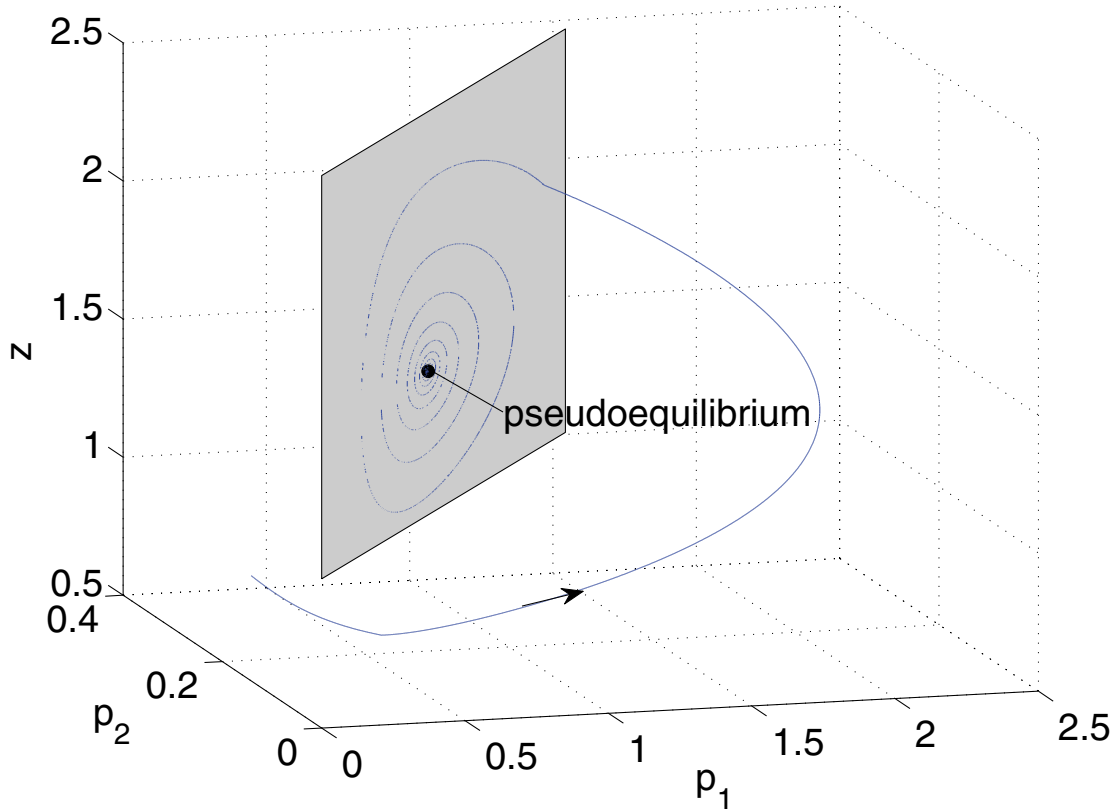


**Figure 3.** Example trajectory of the 1 predator-2 prey model (3.4) for parameter values  $a_q = 4$ ,  $q_1 = 1$ ,  $q_2 = 0.5$ ,  $r_1 = 1.3$ ,  $r_2 = 0.26$ ,  $e = 0.25$ ,  $m = 0.14$ , and  $\beta_1 = \beta_2 = 1$ . The system converges to the pseudoequilibrium (black circle) given by (3.12). The predator's diet is composed of both prey types when the system dynamics evolves along the switching boundary  $h = 0$  (shaded) according to the sliding vector field (3.10).

$\lambda_2 \approx 1.4 \cdot 10^{-3}$ , and  $\lambda_3 \approx 3 \cdot 10^{-4}$ .

**3.3.3. Adding-sliding periodic orbit.** For  $a_q < q_2/q_1$ , the pseudoequilibrium (3.12) of the sliding flow is repelling because the complex conjugate pair of eigenvalues  $\lambda_{1,2}$  have negative real part. The sliding vector field (3.10) behaves as a source (because  $\nabla \cdot f_s|_{(\tilde{p}_1, \tilde{p}_2, \tilde{z})} > 0$ ). There is also a periodic orbit. From our analytical calculations, we know that the vector field  $f_+$  has a cubic tangency with the switching boundary at the cusp at  $(p_1, p_2, z) = (m/(eq_1), m/(eq_1 a_q), r_1 - r_2)$ . Because of the cusp, the local flow near the tangency forces the trajectory of the periodic orbit to first leave the switching boundary tangentially and then to return to it. In doing this, the periodic orbit acquires a nonsliding segment before returning to the switching manifold  $h = 0$ . See Figure 5 for an example trajectory.

One can detect adding-sliding periodic orbits using the sliding condition, as there are two separate pieces of sliding trajectories when  $p_1/(a_q p_2) = 1$ . Between the sliding pieces, there is a nonsliding segment when  $p_1/(a_q p_2) > 1$ . Using numerical simulations of (3.4), we examine

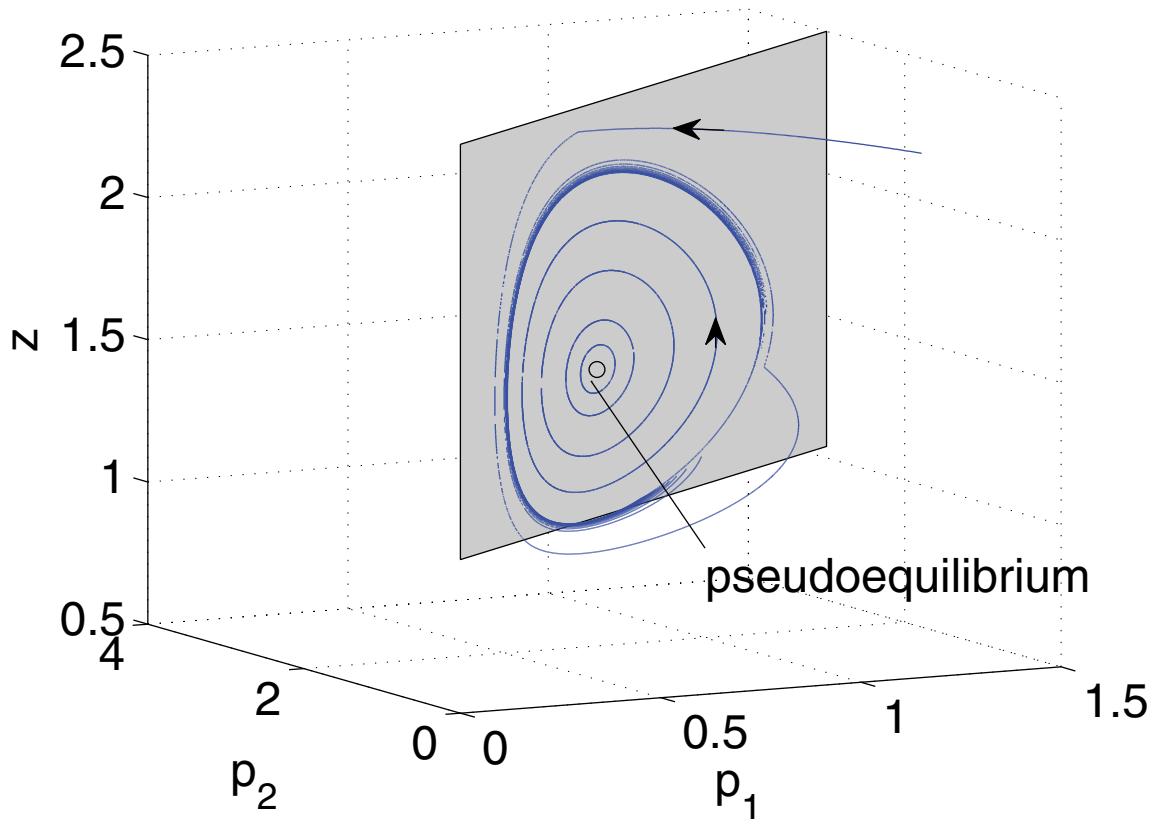


**Figure 4.** Example trajectory of (3.4) for parameter values  $a_q = 0.5$ ,  $q_1 = 1$ ,  $q_2 = 0.5$ ,  $r_1 = 1.3$ ,  $r_2 = 0.26$ ,  $e = 0.25$ ,  $m = 0.14$ , and  $\beta_1 = \beta_2 = 1$ . The pseudoequilibrium (black circle) is surrounded by periodic orbits that evolve along the switching manifold  $h = 0$  in the stable sliding region (shaded). Periodic orbits that reach the boundary between sliding and crossing eventually converge to the periodic orbit that is tangent to the sliding boundary (blue trajectory).

how the amplitude of the adding-sliding periodic orbit measured from the pseudoequilibrium  $(\tilde{p}_1, \tilde{p}_2, \tilde{z})$  in (3.12) scales with the distance to the bifurcation point  $a_{q_{\text{crit}}} = q_2/q_1$ . For  $a_{q_{\text{crit}}} - a_q < 0.1$ , we record the amplitude as the difference in the maximum and minimum values of  $H - \tilde{H}$ ,  $G - \tilde{G}$ , and  $z - \tilde{z}$ , where

$$H = p_1 - a_q p_2, \quad \tilde{H} = \tilde{p}_1 - a_q \tilde{p}_2, \quad G = a_q p_1 + p_2, \quad \tilde{G} = a_q \tilde{p}_1 + \tilde{p}_2.$$

Based on visual inspection, the scaling near  $a_{q_{\text{crit}}}$  appears to be linear (see Figure 6), and we note for comparison that a linear scaling relation is known to arise for the “generalized Hopf bifurcation” for piecewise-smooth dynamical systems discussed in [35]. In this context, such a generalized Hopf bifurcation refers to a periodic orbit that is born when an equilibrium point of a planar, piecewise-smooth continuous system crosses the switching boundary. We note that the word “continuous” is used to describe piecewise-smooth systems with a degree of smoothness of 2 or higher in which the trajectories always cross the switching boundary

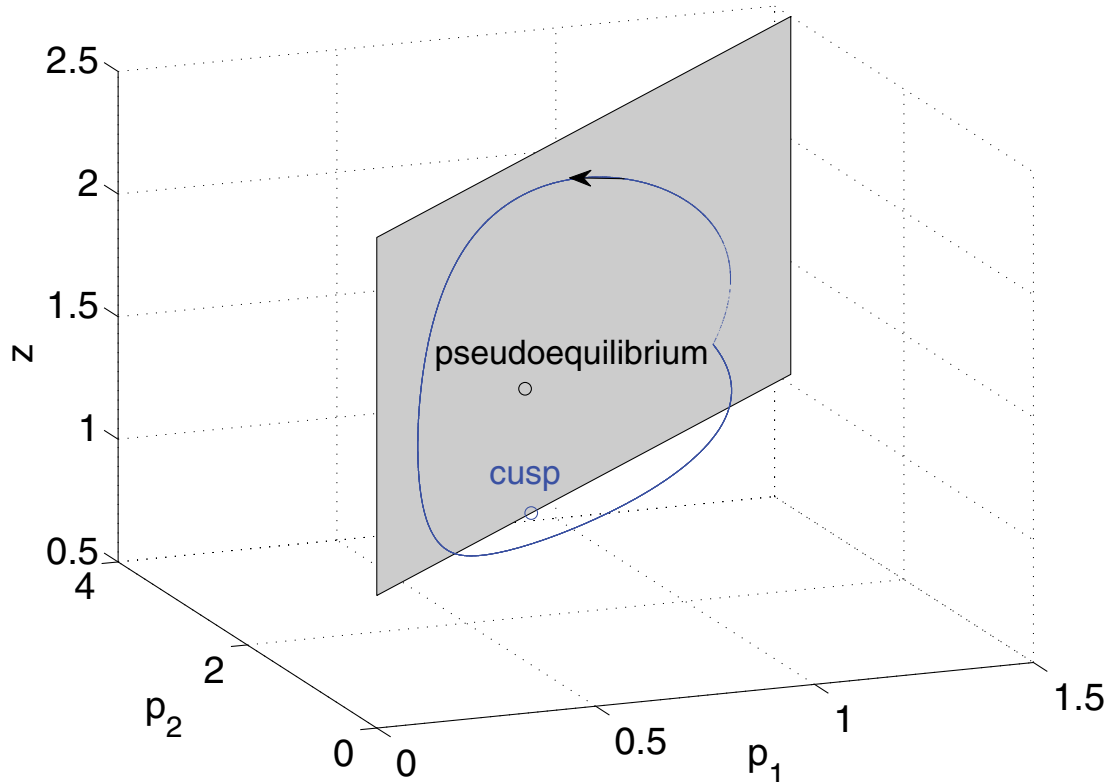


**Figure 5.** Example trajectory of (3.4) for  $a_q = 0.4$ ,  $q_1 = 1$ ,  $q_2 = 0.5$ ,  $r_1 = 1.3$ ,  $r_2 = 0.26$ ,  $e = 0.25$ ,  $m = 0.14$ , and  $\beta_1 = \beta_2 = 1$ . The system has a periodic orbit that leaves the switching manifold (the stable sliding region is shaded) and returns to it because of a cubic tangency between  $f_+$  and the switching manifold. Most of the time, the predator's diet consists of both prey types because the system's dynamics evolves along the switching boundary according to the sliding vector field (3.10). With these parameter values, the adding-sliding periodic orbit has a period of approximately 20 days. In a single cycle, the alternative prey is excluded from the diet and  $p_1/(a_q p_2) > 1$  for approximately 5.5 days.

without evolving along it [5]. In that generalized Hopf bifurcation, a complex conjugate pair of eigenvalues of a piecewise-linear system (which is obtained by linearizing a piecewise-smooth system) have a negative real part on one side of the switching boundary, a zero real part on the switching boundary, and a positive real part on the other side of the switching boundary [35]. We also note that in a similar bifurcation in three-dimensional piecewise linear systems—namely, in the focus-center-limit cycle bifurcation—the amplitude of the limit cycle scales as  $d^{2/3}$ , where  $d$  is the distance from the bifurcation point [14].

The bifurcation in (3.4), in which an adding-sliding periodic orbit arises from a center, has not (to our knowledge) been studied previously. Because a center transitions to such a two-part periodic orbit, we call this a *center to two-part periodic orbit (“C2PO”) bifurcation*. In the C2PO bifurcation, adding-sliding periodic orbits are born via a two-event sequence. First, there is a bifurcation reminiscent of the standard Hopf bifurcation from smooth dynamical

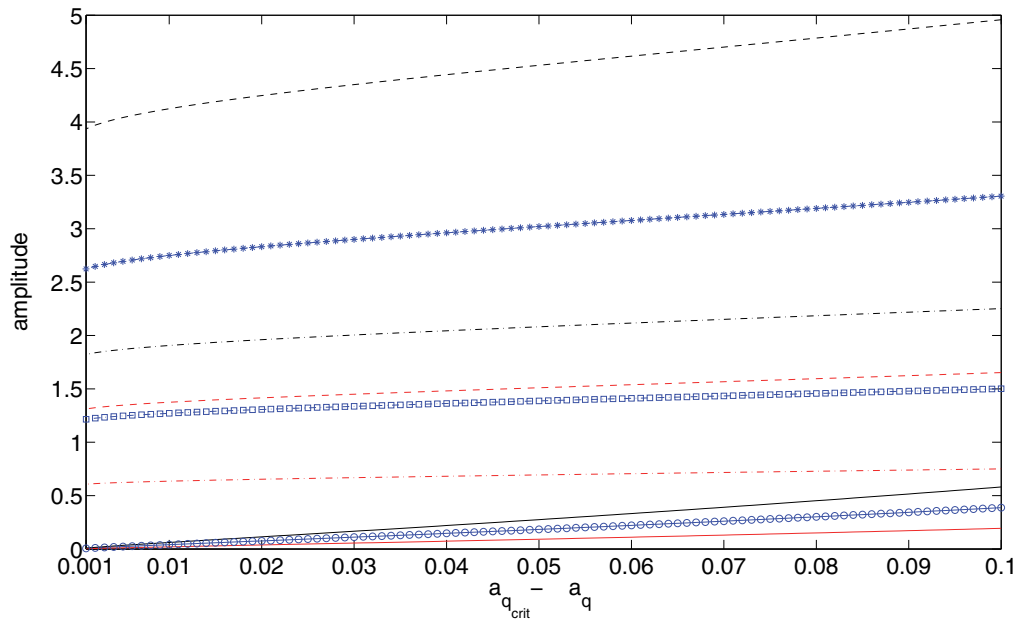


**Figure 6.** Amplitude of  $H - \tilde{H}$  (circles),  $G - \tilde{G}$  (squares), and  $z - \tilde{z}$  (asterisks) of (3.4) [for parameter values  $q_1 = 1$ ,  $q_2 = 0.5$ ,  $r_1 = 1.3$ ,  $r_2 = 0.26$ ,  $e = 0.25$ ,  $m = 0.14$ , and  $\beta_1 = \beta_2 = 1$ ] versus the distance  $a_{q_{\text{crit}}} - a_q < 0.1$  from the bifurcation point  $a_{q_{\text{crit}}} = q_2/q_1$ . We illustrate the possible scaling relations for  $a(H - \tilde{H})$  (solid curves),  $a(G - \tilde{G})$  (dashed curves), and  $a(z - \tilde{z})$  (dash-dotted curves) for three different values of the amplitude scaling:  $a = 1$  (blue),  $a = 0.5$  (red), and  $a = 1.5$  (black).

systems. This arises via the behavior of the eigenvalues of the sliding vector field  $f_s$ , as the pseudoequilibrium changes from attracting to repelling and a periodic orbit appears. Second, as the distance to the bifurcation point increases, the periodic orbit grows and an adding-sliding bifurcation ensues [5].

The C2PO bifurcation satisfies all four of the nondegeneracy conditions for an adding-sliding bifurcation [5]. Indeed, the C2PO bifurcation resembles the standard adding-sliding bifurcation, in which a periodic orbit with a sliding segment and a nonsliding segment is born from an entirely sliding periodic orbit, but the way in which the periodic orbit is born is not quite the same. In contrast to the standard adding-sliding bifurcation, the C2PO bifurcation includes a family of entirely sliding centers (which we have proven are closed curves) at the bifurcation point. The standard adding-sliding bifurcation has only one entirely sliding periodic orbit that grows to encompass a nonsliding segment as the distance from the bifurcation point increases [5].

**3.3.4. Period doubling.** We compute a bifurcation diagram for (3.4) by determining the local maxima of the quantity  $p_1/(a_q p_2) > 1$  when  $a_q \rightarrow 0$  and  $b_q \rightarrow q_2$ . The period-1 adding-sliding periodic orbit that emerges when  $a_q < q_2/q_1$  period-doubles as we decrease  $a_q$  from the bifurcation point. As we illustrate in Figure 7 (see Figure 8 for example trajectories and sliding segments of period-2, period-4, and chaotic orbits), this suggests that there is a cascade to chaos as  $a_q \rightarrow 0$ . From a biological perspective,  $a_q \rightarrow 0$  corresponds to the situation in

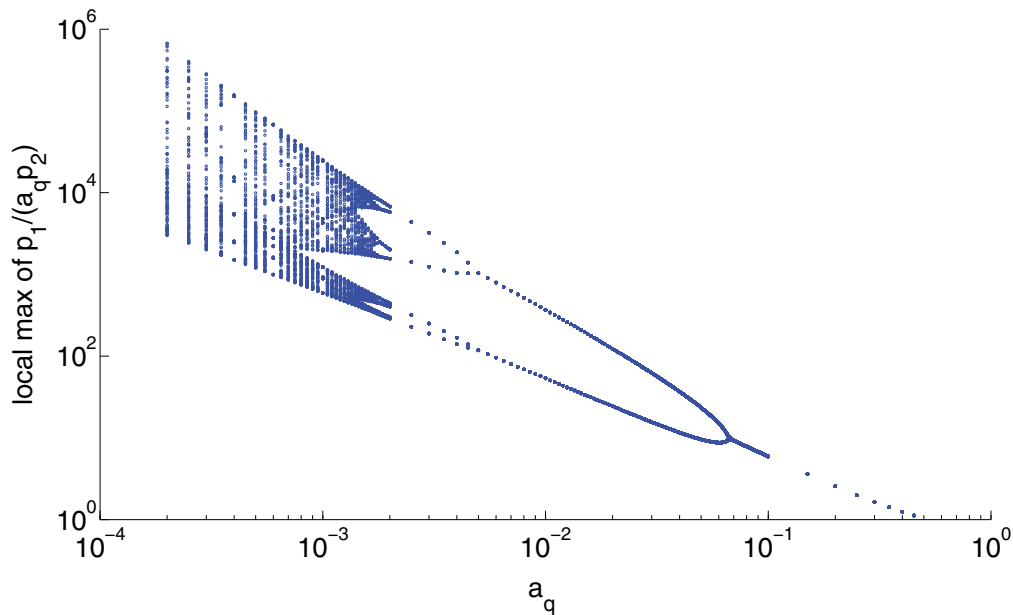


**Figure 7.** Local maxima of  $p_1/(a_q p_2) > 1$  as  $a_q \rightarrow 0$  for (3.4) with parameter values  $r_1 = 1.3$ ,  $r_2 = 0.26$ ,  $e = 0.25$ ,  $m = 0.14$ , and  $\beta_1 = \beta_2 = 1$ .

which there is little decrease in the preference towards the alternative prey if the predator has an increase in specialization towards the preferred prey.

**3.4. Comparison of 1 predator-2 prey model simulations and planktonic protozoa-algae data.** In this section, we compare the prey ratio of adding-sliding period-1 and period-2 orbits from the 1 predator-2 prey model (3.4) with data on cryptophyte and diatom prey collected from Lake Constance in spring. We choose to compare the scaled prey ratio  $p_1/(a_q p_2)$  predicted by the model with the scaled prey ratio calculated from the data because  $p_1/(a_q p_2) = 1$  indicates when the dynamics of the 1 predator-2 prey system (3.4) are governed by the sliding vector field (3.10) at the switching boundary. We use an approximate Bayesian computation scheme [45] to fit the prey growth rates and the predator mortality rate to the periodicity exhibited in the data. In the numerical simulations of (3.4), we choose values for these three parameters from the ranges suggested by our fitting results. For the other parameters, we choose values that illustrate the mathematical properties of the model. Thus, the latter set of parameter values are arbitrary and are not necessarily representative of the biological properties of the species groups that we include in our comparison.

Previous studies of the Lake Constance data set suggest that ciliates are the most abundant herbivorous zooplankton group in spring, whereas cryptophytes and diatoms are the dominant species groups in the phytoplankton community [43]. Our motivation to compare the data and our prey-switching model is the observed prey preference among ciliate species that actively select against diatom prey when offered a mixed diet of both cryptophytes and diatom prey [31]. We restrict the time window of comparison to spring, as it has been sug-

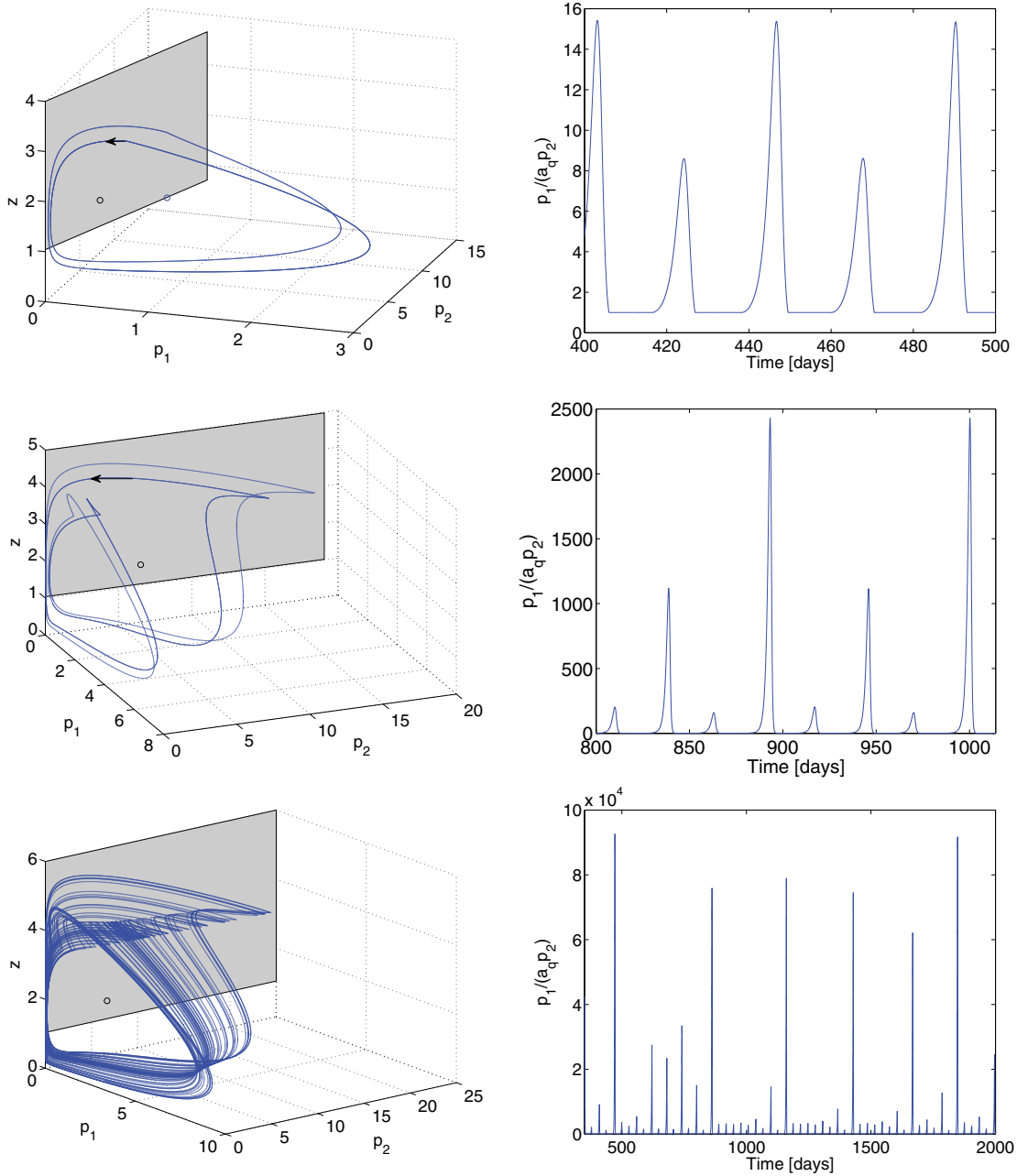


**Figure 8.** (Left) Example trajectories and (right) scaled prey ratio  $p_1/(a_q p_2)$  of (3.4) with (top)  $a_q = 0.06$ , (middle)  $a_q = 0.0035$ , and (bottom)  $a_q = 0.0005$  for the parameter values  $q_1 = 1$ ,  $q_2 = 0.5$ ,  $r_1 = 1.3$ ,  $r_2 = 0.26$ ,  $e = 0.25$ ,  $m = 0.14$ , and  $\beta_1 = \beta_2 = 1$ .

gested that predator-prey feeding interactions are then an important factor in explaining the ciliate-algal dynamics in Lake Constance [44]. Moreover, it is also believed that in the spring such interactions have larger relative importance than environmental conditions [36].

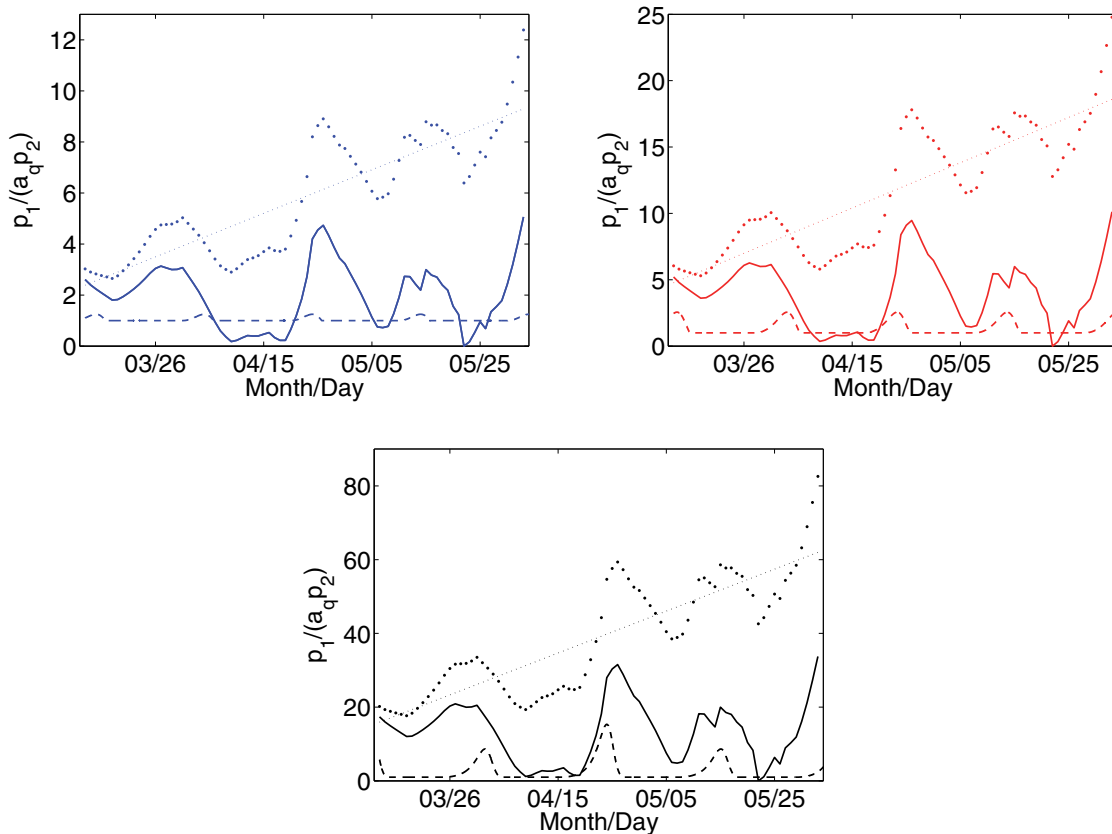


**Figure 9.** (Dashed curves) Scaled prey ratio  $p_1/(a_q p_2)$  for simulations of (3.4) [for parameter values  $r_1 = 1.3$ ,  $r_2 = 0.26$ ,  $e = 0.25$ ,  $m = 0.14$ , and  $\beta_1 = \beta_2 = 1$ ]; (points) mean data calculated for the scaled prey ratio  $p_1/(a_q p_2)$  in spring in Lake Constance over the period 1979–1999; and (solid curves) processed data. The prey ratios are scaled by (top left)  $a_q = 0.4$ , (top right)  $a_q = 0.2$ , and (bottom)  $a_q = 0.06$ . For each panel, we obtain the processed data by subtracting a least-squares fit of a straight line (dotted lines) to the means of the data. The equations for these lines are (top left)  $y = 0.0853x + 2.3872$ , where the norm of the residuals is 10.9685; (top right)  $y = 0.1706x + 4.7743$ , where the norm of the residuals is 21.9370; and (bottom)  $y = 0.5686x + 15.9144$ , where the norm of the residuals is 73.1235. We then rescale the detrended data to have a minimum of 0. The preferred prey  $p_1$  is composed of data for *Cryptomonas ovata*, *Cryptomonas marssonii*, *Cryptomonas reflexa*, *Cryptomonas erosa*, *Rhodomonas lens*, and *Rhodomonas minuta*. The alternative prey group  $p_2$  is composed of data for small and medium-size *Chlamydomonas* spp. and *Stephanodiscus parvus*. These data, which were previously reported in [41, 42], were provided by Ursula Gaedke.

We use six different cryptophyte species as the group of preferred prey and three different diatoms species to represent the ciliates' alternative prey. We include data for phytoplankton whose cell size is sufficiently small compared to the size of ciliate predators and which dominate the algal community in Lake Constance in spring [43]. For both species groups, we use linear interpolation to obtain intermediate biomass values for each day of the year from approximately biweekly measurements. We then calculate the mean of the 20 interpolated yearly data between 1979 and 1999. These data exhibit an increasing trend. We remove the trend by subtracting a least-squares fit of a straight line from the data. In Figure 9, we compare these

data with the prey ratio that we obtain from simulations of (3.4). Although our model does not capture the increasing trend, it successfully reproduces the periodic pattern early in the growing season when one can argue that predator-prey interactions govern the protist-algae dynamics more than physical driving forces in water masses that are rich in nutrients [36].

**4. Discussion.** We have combined adaptive predator behavior and ecological trade-offs to model the dynamics of a predator that feeds on a preferred and alternative prey as a piecewise-smooth dynamical system. Our model describes a predator that can adaptively change its diet depending on the abundances of its preferred and alternative prey. We assumed a linear trade-off in prey preference and analyzed the dynamics of the system as we adjusted the slope of the trade-off. To compensate for the preference, we assumed that the preferred prey has a larger growth rate than the alternative prey.

Our model predicts a steady state for the predator and prey populations as long as the trade-off in prey preference is sufficiently steep. In other words, a steady state occurs when a small increase in specialization towards the preferred prey would result in a large decrease in how much energy the predator could gain from the alternative prey. As we decrease the slope of the preference trade-off, a periodic orbit appears and period-doubles as the slope approaches 0. After the bifurcation, the population densities oscillate and the prey ratio is no longer constant. From a biological perspective, a mild trade-off suggests that a predator with a small increase in the energy gained from the preferred prey would exhibit only a small decrease in the energy gained from the alternative prey. In the present paper, we considered a linear preference trade-off as a first step towards studying the effect of such a trade-off in a predator-prey interaction in which prey switching occurs. Although several studies and observations support the existence of trade-offs [22, 30], it is not clear what kind of functional form they take. A previous model for population dynamics and prey switching studied a convex (i.e., concave down) trade-off between the attack rate and the degree of specialization exhibited by a predator [2]. Concave relationships have been formulated for the consumption of two prey species and the energy obtained from two prey species in an approach in which these functions are plotted in the same picture in order to solve the problem of optimal diet [34]. To develop a more complete understanding of the effects of a preference trade-off on populations dynamics, it would be useful to consider generalizations of our model with nonlinear trade-off functions.

In the present paper, we have interpreted adaptation as flexible feeding behavior of a predator that has two feeding modes for consuming its preferred prey, and we have assumed that it can switch between them in response to prey densities. Recent studies have shown that rapid adaptation of traits affects ecological interactions and can be observed especially in organisms with short lifespans, such as species in plankton communities [4, 21]. Interactions between evolutionary adaptation and population dynamics have been studied using both a framework of *fast-slow dynamical systems* and *slow-fast dynamical systems*. The former approach has given insight into how evolution of traits arises in population dynamics by studying the limit in which trait evolution occurs on a much faster time scale than predator-prey interactions [10]. In the latter framework, the consequences that ecological dynamics can have on the evolution of traits have been studied using piecewise-smooth dynamical systems; this assumes that evolution occurs on a much longer time scale than predator-prey interactions [11]. Formulating a fast-slow dynamical-system analogue of (3.4) would enable an interesting

comparison of piecewise-smooth and fast-slow dynamical systems and should be insightful for modeling interactions between change in feeding behavior (or evolutionary adaptation) and population dynamics. Currently, we are considering a fast-slow dynamical system with three slow variables [the population densities of the predator ( $z$ ), preferred prey ( $p_1$ ), and alternative prey ( $p_2$ )] and one fast variable [the extent of preference towards the preferred prey ( $q_1$ )] to describe a predator that feeds adaptively on its preferred and alternative prey. This fast-slow system takes the form

$$(4.1) \quad \begin{aligned} \dot{p}_1 &= f_1(p_1, p_2, z, q_1), \\ \dot{p}_2 &= f_2(p_1, p_2, z, q_1), \\ \dot{z} &= f_3(p_1, p_2, z, q_1), \\ \epsilon \dot{q}_1 &= g_1(p_1, p_2, z, q_1), \end{aligned}$$

where  $\epsilon \ll 1$  indicates the difference in time scales between population dynamics and predator preference.

In the present paper, we chose to use exponential prey growth to simplify analytical calculations. An important generalization is to consider logistic prey growth, as nutrient limitation is one of the most important nonliving factors that can drive the temporal pattern of phytoplankton growth [37]. However, it has been suggested that the importance of nutrient limitation is less pronounced than protist grazing at the beginning of a growth season [36] for water masses that are rich in nutrients. Although considering logistic prey growth increases the number of parameters in the model (in addition to making analytical calculations significantly more challenging), it has two key advantages: (1) it would expand the suitable time window for comparing simulations with data in water masses that are rich in nutrients; and (2) its less restrictive assumptions yield a model that is also reasonable in principle for water masses with low nutrient levels [36].

Our 1 predator-2 prey system (3.4) describes a feeding interaction in which there is a known predator preference and in which there is active selection against an alternative prey. This model reproduces the periodicity in the scaled prey ratio during the early growing season in Lake Constance, during which predator-prey interaction has been suggested as an important driving factor for ciliate-algae dynamics. However, it does not capture the increasing trend in the data. We speculate that a generalization of our model that allows the prey growth to increase slowly in time might make it possible to also capture the increasing trend. We motivate the time-dependent prey growth rate by the fact that the phytoplankton production-to-biomass ratio calculated for Lake Constance exhibits a linear increase in the prey growth in spring and a decrease in autumn [15]. Scaling the prey ratio by the time since the start of spring would then allow us to test whether growth is slowly increasing over the length of the growing season.

As a first step towards studying models of adaptive predator behavior and ecological trade-offs, we started from the simplest case (i.e., a system with one predator and two prey). In the model (3.4) that we have introduced, functional diversity is present only in the prey community and it arises as the difference in prey growth rates. Accordingly, we have chosen species from a large data set to consider representative prey groups and have left prey competition and predator diversity for future work. Ciliates are known to have different modes of predator behavior, and they can be categorized roughly in terms of being more or less

selective [49]. To illustrate a predator that is more selective, we note that some ciliate species hunt as “interception feeders” that scavenge on food particles and intercept them directly. By contrast, ciliate “filter feeders” sieve suspended food particles and provide an example of less selective predators. One can represent such diversity in the predator community using different preference trade-offs. This could be studied using a piecewise-smooth dynamical system with more than three dimensions (or by using a fast-slow dynamical system) and which could have more than one switching manifold. Moreover, the switching manifolds might intersect with each other. Such a generalization would thus be very interesting (and challenging) to study from both biological and mathematical perspectives. We have already motivated the former perspective. From a mathematical viewpoint, we remark that there does not yet exist a general treatment for bifurcations in piecewise-smooth dynamical systems that arise from intersections of switching manifolds when the ambient space has more than three dimensions [9].

Our model exhibits a novel (so-called C2PO) bifurcation, in which the dynamics transitions at the bifurcation point between convergence to a pseudoequilibrium and periodic adding-sliding oscillations through a center. This emergence of adding-sliding orbits differs from the usual way that they emerge in piecewise-smooth dynamical systems [5]. The standard mechanism entails the birth of an adding-sliding periodic orbit following a bifurcation in which the eigenvalues of the pseudoequilibrium cross the imaginary axis, so that the pseudoequilibrium changes from attracting to repelling and an entirely sliding periodic orbit is born. As the amplitude of the periodic orbit (which lies entirely on the switching boundary) grows, the sliding periodic orbit eventually becomes tangent to the boundary between sliding and crossing. Finally, this periodic orbit becomes a trajectory that has a sliding segment separated by a nonsliding segment [5]. We observed numerically that the amplitude scaling of the adding-sliding periodic orbit that emerges from the C2PO bifurcation appears to be linear in the distance from the bifurcation, which is also the case for the generalized Hopf bifurcation in piecewise-smooth dynamical systems in [35].

**5. Conclusions.** We combined two ecological concepts—prey switching and trade-offs—and used the framework of piecewise-smooth dynamical systems to develop a model of one predator that feeds on a preferred and an alternative prey. We derived analytical expressions for the pseudoequilibrium, its eigenvalues, and the points for tangencies between the two vector fields and the switching boundary. We confirmed our analytical results using numerical simulations, and we discovered a novel bifurcation in which an adding-sliding periodic orbit is born from a center. Based on numerical simulations close to the bifurcation point, the amplitude of the adding-sliding periodic orbit seems to scale linearly with the distance from the bifurcation point.

Our model introduces a way to link trade-offs with adaptive predator behavior. We compared the results of our simulations with data on freshwater plankton, but we remark that similar prey-switching models can also be formulated for any other 1 predator-2 prey interaction in which it is viable to use models based on low-dimensional differential equations (i.e., large population size, well-mixed environment, and the use of community-integrated parameters). We also discussed several biologically motivated generalizations of our model. We believe that our current model and these generalizations provide promising directions for

examining possible mechanisms for ecological trade-offs in population dynamics.

Although we have motivated our investigation primarily from an ecological perspective, it is also important to stress the utility of our model for development of new theoretical understanding in piecewise-smooth dynamical systems. The ecological and mathematical motivations complement each other very well, and investigating the condition for sliding corresponds to studying a scaled prey ratio, and this in turn offers a possible link between ecological trade-offs and population dynamics. We believe that our model offers an encouraging example of how combining theoretical and practical perspectives can give new insights both for the development of theory of piecewise-smooth dynamical systems as well as for the development of models of population dynamics with predictive power.

**Acknowledgments.** We thank Jorn Bruggeman, Alan Champneys, Jon Chapman, Stephen Ellner, John Guckenheimer, John Hogan, Christian Kuehn, John Norbury, and Tere Seara for helpful discussions. We thank Ursula Gaedke for useful discussions and sending us data, and we thank Chris Klausmeier and Mike Jeffrey for numerous helpful discussions and comments. We also thank the anonymous referees for their constructive and thorough feedback and the editor for comments that helped immensely to improve this paper.

#### REFERENCES

- [1] P. A. ABRAMS AND H. MATSUDA, *Positive indirect effects between prey species that share predators*, Ecology, 77 (1996), pp. 610–616.
- [2] P. A. ABRAMS AND H. MATSUDA, *Population dynamical consequences of reduced predator switching at low total prey densities*, Popul. Ecol., 45 (2003), pp. 175–185.
- [3] E. BÄURLE AND U. GAEDKE, EDS., *Lake Constance — Characterization of an Ecosystem in Transition*, Adv. Limnol. 53, Schweizerbart Science Publishers, Stuttgart, Germany, 1999.
- [4] L. BECKS, S. P. ELLNER, L. E. JONES, AND N. G. HAIRSTON, JR., *Reduction of adaptive genetic diversity radically alters eco-evolutionary community dynamics*, Ecol. Lett., 13 (2010), pp. 989–997.
- [5] M. DI BERNARDO, C. J. BUDD, A. R. CHAMPNEYS, AND P. KOWALCZYK, *Piecewise-Smooth Dynamical Systems*, Springer, London, 2008.
- [6] D. S. BOUKAL AND V. KRIVAN, *Lyapunov functions for Lotka-Volterra predator-prey models with optimal foraging behavior*, J. Math. Biol., 39 (1999), pp. 439–517.
- [7] G. CASEY, H. DE JONG, AND J.-L. GOUZÉ, *Piecewise-linear models of genetic regulatory networks: Equilibria and their stability*, J. Math. Biol., 52 (2006), pp. 27–56.
- [8] A. R. CHAMPNEYS AND M. DI BERNARDO, *Piecewise smooth dynamical systems*, Scholarpedia, 3 (9) (2008), 4041.
- [9] A. COLOMBO, M. DI BERNARDO, S. J. HOGAN, AND M. R. JEFFREY, *Bifurcations of piecewise smooth flows: Perspectives, methodologies and open problems*, Phys. D, 241 (2012), pp. 1845–1860.
- [10] M. H. CORTEZ AND S. P. ELLNER, *Understanding rapid evolution in predator-prey interactions using the theory of fast-slow dynamical systems*, Am. Nat., 176 (2010), pp. E109–E127.
- [11] F. DERCOLE, F. FERRIÈRE, A. GRAGNANI, AND S. RINALDI, *Coevolution of slow-fast populations: Evolutionary sliding, evolutionary pseudo-equilibria and complex Red Queen dynamics*, P. Roy. Soc. Lond. B, 273 (2006), pp. 983–990.
- [12] F. DERCOLE, A. GRAGNANI, AND S. RINALDI, *Bifurcation analysis of piecewise-smooth ecological models*, Theor. Pop. Biol., 72 (2007), pp. 197–213.
- [13] A. F. FILIPPOV, *Differential Equations with Discontinuous Righthand Sides*, Kluwer Academic Publishers, Dordrecht, The Netherlands, 1988.
- [14] E. FREIRE, E. PONCE, AND J. ROS, *The focus-center-limit cycle bifurcation in symmetric 3D piecewise linear systems*, SIAM J. Appl. Math., 65 (2005), pp. 1933–1951.
- [15] U. GAEDKE, *private communication*, 2012.

- [16] G. F. GAUSE, N. P. SMARAGDOVA, AND A. A. WITT, *Further studies of interaction between predators and prey*, J. Anim. Ecol., 5 (1936), pp. 1–18.
- [17] L. GLASS, *Classification of biological networks by their qualitative dynamics*, J. Theoret. Biol., 54 (1975), pp. 85–107.
- [18] V. GOVORUKHIN, *Calculation Lyapunov Exponents for ODE*, MATLAB Central File Exchange, 2004, retrieved November 15, 2013.
- [19] C. S. HOLLING, *The functional response of predators to prey density and its role in mimicry and population regulation*, Mem. Entomol. Soc. Can., 45 (1965), pp. 1–60.
- [20] M. R. JEFFREY AND S. J. HOGAN, *The geometry of generic sliding bifurcations*, SIAM Rev., 53 (2011), pp. 505–525.
- [21] L. E. JONES, L. BECKS, S. P. ELLNER, N. G. HAIRSTON, JR., T. YOSHIDA, AND G. F. FUSSMAN, *Rapid contemporary evolution of clonal food web dynamics*, Philos. T. Roy. Soc. B, 364 (2009), pp. 505–525.
- [22] J. M. KNEITEL AND J. M. CHASE, *Trade-offs in community ecology: Linking spatial scales and species coexistence*, Ecol. Lett., 7 (2004), pp. 69–80.
- [23] A. KOROBENIKOV AND G. C. WAKE, *Global properties of the three-dimensional predator-prey Lotka-Volterra*, J. Appl. Math. Decis. Sci., 3 (1999), pp. 155–162.
- [24] V. KRIVAN, *Optimal foraging and predator-prey dynamics I*, Theor. Pop. Biol., 49 (1996), pp. 265–290.
- [25] V. KRIVAN, *Dynamic ideal free distribution: Effects of optimal patch choice on predator-prey dynamics*, Am. Nat., 149 (1997), pp. 167–178.
- [26] V. KRIVAN, *The Lotka-Volterra predator-prey model with foraging-predation risk trade-offs*, Am. Nat., 170 (2007), pp. 771–782.
- [27] V. KRIVAN AND J. EISNER, *Optimal foraging and predator-prey dynamics, III*, Theor. Pop. Biol., 63 (2003), pp. 269–279.
- [28] V. KRIVAN AND A. SIKDER, *Optimal foraging and predator-prey dynamics II*, Theor. Pop. Biol., 55 (1999), pp. 111–126.
- [29] Y. A. KUZNETSOV, S. RINALDI, AND A. GRAGNANI, *One-parameter bifurcations in planar Filippov systems*, Internat. J. Bifur. Chaos Appl. Sci. Engrg., 13 (2003), pp. 2157–2188.
- [30] E. LITCHMAN AND C. A. KLAUSMEIER, *Trait-based community ecology of phytoplankton*, Annu. Rev. Ecol. Evol. Syst., 39 (2008), pp. 615–639.
- [31] H. MÜLLER AND A. SCHLEGEL, *Responses of three freshwater planktonic ciliates with different feeding modes to cryptophyte and diatom prey*, Aquat. Microb. Ecol., 17 (1999), pp. 49–60.
- [32] W. W. MURDOCH, *Switching in general predators: Experiments on prey specificity and stability of prey populations*, Ecol. Monog., 39 (1969), pp. 335–354.
- [33] P. PIROINEN AND Y. A. KUZNETSOV, *An event-driven method to simulate Filippov systems with accurate computing of sliding motions*, ACM Trans. Math. Software, 34 (2008), pp. 13:1–13:24.
- [34] D. J. RAPPORT, *An optimization model of food selection*, Am. Nat., 105 (1971), pp. 575–587.
- [35] D. J. W. SIMPSON AND J. D. MEISS, *Andronov-Hopf bifurcations in planar, piecewise-smooth, continuous flows*, Phys. Lett. A, 371 (2007), pp. 213–220.
- [36] U. SOMMER, R. ADRIAN, L. DE SENERPONT DOMIS, J. J. ELSER, U. GAEDKE, B. IBELINGS, E. JEPPESEN, M. LURLING, J. C. MOLINERO, W. M. MOOIJ, E. VAN DONK, AND M. WINDER, *Beyond the Plankton Ecology Group (PEG) model: Mechanisms driving plankton succession*, Annu. Rev. Ecol. Evol. Syst., 43 (2012), pp. 429–448.
- [37] U. SOMMER, Z. M. GLIWICZ, W. LAMPERT, AND A. DUNCAN, *The PEG-model of seasonal succession of planktonic events in freshwaters*, Arch. Hydrobiol., 106 (1986), pp. 433–471.
- [38] D. W. STEPHENS AND J. R. KREBS, *Foraging Theory*, Princeton University Press, Princeton, NJ, 1986.
- [39] J. SUN, E. M. BOLLT, M. A. PORTER, AND M. S. DAWKINS, *A mathematical model for the dynamics and synchronization of cows*, Phys. D, 240 (2011), pp. 1497–1509.
- [40] E. TERAMOTO, K. KAWASAKI, AND N. SHIGESADA, *Switching effect of predation on competitive prey species*, J. Theoret. Biol., 79 (1979), pp. 303–315.
- [41] K. TIROK AND U. GAEDKE, *Spring weather determines the relative importance of ciliates, rotifers and crustaceans for the initiation of the clear-water phase in a large, deep lake*, J. Plankton Res., 28 (2006), pp. 361–373.
- [42] K. TIROK AND U. GAEDKE, *The effect of irradiance, vertical mixing and temperature on spring phytoplankton dynamics under climate change: Long-term observations and model analysis*, Oecologia, 150

- (2007), pp. 625–642.
- [43] K. TIROK AND U. GAEDKE, *Regulation of planktonic ciliate dynamics and functional composition during spring in Lake Constance*, *Aquat. Microb. Ecol.*, 49 (2007), pp. 87–100.
- [44] K. TIROK AND U. GAEDKE, *Internally driven alternation of functional traits in a multispecies predator-prey system*, *Ecology*, 91 (2010), pp. 1748–1762.
- [45] T. TONI, D. WELCH, N. STRELKOWA, A. IPSEN, AND M. P. H. STUMPF, *Approximate Bayesian computation scheme for parameter inference and model selection in dynamical systems*, *J. Roy. Soc. Interface*, 6 (2009), pp. 187–202.
- [46] V. I. UTKIN, *Sliding Modes in Control and Optimization*, Springer-Verlag, Berlin, 1992.
- [47] E. VAN LEEUWEN, Å. BRÄNNSTRÖM, V. A. A. JANSEN, U. DIECKMANN, AND A. G. ROSSBERG, *A generalized functional response for predators that switch between multiple prey species*, *J. Theoret. Biol.*, 328 (2013), pp. 89–98.
- [48] E. VAN LEEUWEN, V. A. A. JANSEN, AND P. W. BRIGHT, *How population dynamics shape the functional response in a one-predator-two-prey system*, *Ecology*, 88 (2007), pp. 1571–1581.
- [49] P. VERITY, *Feeding in planktonic protozoans: Evidence for nonrandom acquisition of prey*, *J. Protozool.*, 38 (1991), pp. 69–76.
- [50] A. WOLF, J. B. SWIFT, H. L. SWINNEY, AND J. A. VASTANO, *Determining Lyapunov exponents from a time series*, *Phys. D*, 16 (1985), pp. 285–317.